JB
Journals.ASM.org

Physiology of Resistant *Deinococcus geothermalis* Bacterium Aerobically Cultivated in Low-Manganese Medium

Christina Liedert,[a]* Minna Peltola,[b]* Jörg Bernhardt,[c] Peter Neubauer,[a]* and Mirja Salkinoja-Salonen[b]

Bioprocess Engineering Laboratory, Department of Process and Environmental Engineering, University of Oulu, Oulu, Finland[a]; Division of Microbiology, Department of Food and Environmental Sciences, University of Helsinki, Helsinki, Finland[b]; and Institute for Microbiology, Ernst-Moritz-Arndt-Universität Greifswald, Greifswald, Germany[c]

This dynamic proteome study describes the physiology of growth and survival of *Deinococcus geothermalis*, in conditions simulating paper machine waters being aerobic, warm, and low in carbon and manganese. The industrial environment of this species differs from its natural habitats, geothermal springs and deep ocean subsurfaces, by being highly exposed to oxygen. Quantitative proteome analysis using two-dimensional gel electrophoresis and bioinformatic tools showed expression change for 165 proteins, from which 47 were assigned to a function. We propose that *D. geothermalis* grew and survived in aerobic conditions by channeling central carbon metabolism to pathways where mainly NADPH rather than NADH was retrieved from the carbon source. A major part of the carbon substrate was converted into succinate, which was not a fermentation product but likely served combating reactive oxygen species (ROS). Transition from growth to nongrowth resulted in downregulation of the oxidative phosphorylation observed as reduced expression of V-type ATPase responsible for ATP synthesis in *D. geothermalis*. The battle against oxidative stress was seen as upregulation of superoxide dismutase (Mn dependent) and catalase, as well as several protein repair enzymes, including FeS cluster assembly proteins of the iron-sulfur cluster assembly protein system, peptidyl-prolyl isomerase, and chaperones. Addition of soluble Mn reinitiated respiration and proliferation with concomitant acidification, indicating that aerobic metabolism was restricted by access to manganese. We conclude that *D. geothermalis* prefers to combat ROS using manganese-dependent enzymes, but when manganese is not available central carbon metabolism is used to produce ROS neutralizing metabolites at the expense of high utilization of carbon substrate.

Deinococcus geothermalis belongs to the deeply branched bacterial phylum *Deinococcus-Thermus* (19), which is known for its extremophilic species. *D. geothermalis* and *D. radiodurans* are extremely resistance against infrared (IR) and UV radiation and desiccation (12, 42). *D. geothermalis* was first described as an aerobic bacterium found in geothermal springs (17) and later in deep-ocean subsurfaces (34), showing that it can grow in the absence of oxygen. *D. geothermalis* is able to reduce Fe(III), U(VI), and Cr(VI) and was genetically modified to reduce Hg(II) at elevated temperatures (7). These characteristics make the species a potential candidate for biotechnical applications such as the remediation of nuclear waste lands. The members of the *Deinococcus* family are also screened for biofuel, green chemistry, and antibiotics production purposes.

D. geothermalis has found an industrial niche in paper industry, where it forms biofilms on warm air-exposed splash surfaces (33, 35, 44, 45, 58), showing that this species is able to fight oxidative stress caused by aerobic lifestyle and by oxidizing biocides. The genome of *D. geothermalis* was sequenced (42), but it did not reveal unique defense systems which could be responsible for the extreme resistance of this species, and thus the molecular background of the *D. geothermalis* resistance remains unclear. The availability of *D. geothermalis* genome sequence allowed proteomics analysis, and from the 3,042 protein coding sequences (42) the expression of 299 cytosolic proteins and 25 cell envelope associated proteins were confirmed using two-dimensional gel electrophoresis (2-DE) (38) and 117 membrane-associated proteins with one-dimensional polyacrylamide gel electrophoresis (PAGE) and liquid chromatography-tandem mass spectrometry (53). 2-DE is widely used for the analysis of whole proteomes and has been applied in a number of bacterial global gene expression studies (for examples, see references 10 and 25). Proteomic signatures (55) not only reveal which metabolic pathways are active in cells but may also be used to predict the physiological state of the cells, e.g., in bioreactors and natural ecosystems such as biofilms (26). In the present study, we used 2-DE to describe the physiology of *D. geothermalis* growth and its survival in fully aerobic, warm industrial water simulating an environment such as paper machine recycling waters (45). This is the first functional proteome study of *D. geothermalis* revealing unique features related to adaptation.

MATERIALS AND METHODS

Strain and cultivation conditions. *D. geothermalis* E50051 (HAMBI 2411) was grown in a 3-liter flask, with 500 ml of medium, at 45°C under constant agitation (160 rpm, orbital shaker) with no aeration other than diffusion through the agitated surface. The R2 starch broth contained (per liter) soluble starch, 0.5 g; casein digest. 0.75 g; yeast extract. 0.5 g; K_2HPO_4, 0.3 g; sodium pyruvate. 0.3 g; meat extract. 0.5 g; and $MgSO_4$, 0.024 g (pH 7.0). The redox potential was >100 mV (measured against calomel reference). No manganese was added; the background concentration, <10 μg liter^{-1}, is close to that in paper machine waters (30 μg liter^{-1}), as measured using inductively coupled plasma-optical emission

Received 1 December 2011 Accepted 22 December 2011

Published ahead of print 6 January 2012

Address correspondence to Christina Liedert, christina.liedert@vtt.fi, or Mirja Salkinoja-Salonen, mirja.salkinoja-salonen@helsinki.fi.

* Present address: Christina Liedert, Technical Research Centre of Finland, VTT, Oulu, Finland; Minna Peltola, Department of Chemistry and Bioengineering, Tampere University of Technology, Tampere, Finland; Peter Neubauer, Laboratory of Bioprocess Engineering, Department of Biotechnology, Technische Universität Berlin, Berlin, Germany.

doi:10.1128/JB.06429-11

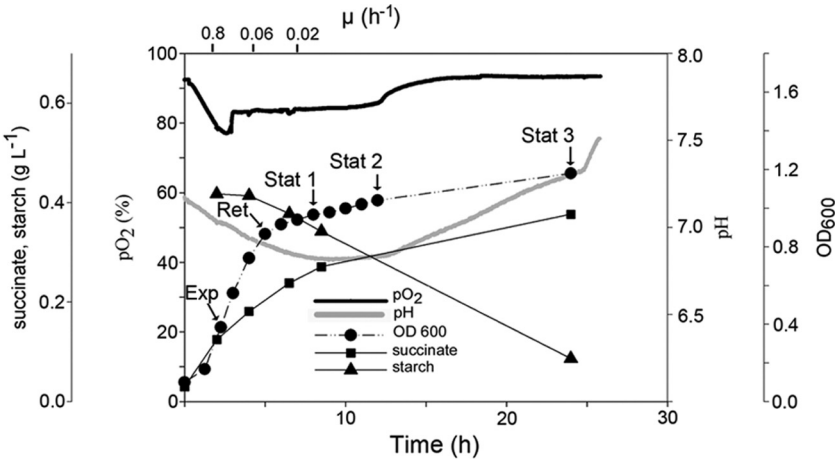

FIG 1 Kinetics of aerobic growth of *D. geothermalis* E50051 at 45°C in low-carbon medium (R2 starch broth, 2.3 g of carbon). The sampling points for the medium and proteome samples are indicated. Aeration was by constant agitation. The dissolved oxygen concentration and pH were measured online. The samples were analyzed for OD_{600}, ethanol, and short-chain carboxylic acids (formic, lactic, acetic, butyric, malic, propionic, valeric, and succinic acid). Succinic acid was the only organic acid detected in the three parallel cultivations.

spectrometry (ICP-OES). The medium was seeded with ca. 1/10 volume of an overnight preculture to an optical density at 600 nm (OD_{600}) of 0.1. The experiments under a modified atmosphere (1% O_2, 1% CO_2, 98% N_2; HERAcell 150i [Thermo Scientific, USA]) were performed with cultures on R2A plates (Lab M, Ltd., Lancashire, United Kingdom) at 45°C for 2 to 3 days. Anaerobic cultivation was performed in an anaerobic chamber (2.5 liters) using Anerocult A (Merck KGaA, Darmstadt, Germany) bags to create anaerobicity, verified with indicator chips (Microbiologiga Anaerotest; Merck KGaA). To test for alternate electron acceptors R2A (Lab M) plates were overlaid with 3-ml layers of agar per plate containing one of the following: 0.5 g of iron powder liter^{-1} or MnO_2 or KNO_3 (20 mM each).

pH and pO_2 measurement. Dissolved oxygen (pO_2) and pH were measured online with a wireless system (Senbit; teleBITcom GmbH, Teltow, Germany) from a 1-liter shake flask containing 100 ml of medium. The oxygen sensors were calibrated prior to each experiment by immersion in 3% (wt/vol) aqueous Na_2SO_3 for $pO_2 = 0$.

Medium composition analysis. The cells were removed by centrifugation (13,100 × *g*, 10 min, 4°C). The starch content in the supernatant was analyzed with a YSI 2700 Select Biochemical Analyzer (YSI, Inc., Yellow Springs, OH) after acid hydrolysis (1 volume of 2 M HCl solution for 2 h at 95°C), neutralized (1 volume of 2 M NaOH) and buffered to pH 7.0 (by adding 1 volume of 0.5 M potassium phosphate). For the determination of volatile acids (acetic, formic, lactic, butyric, malic, propionic, valeric, and succinic acids) and ethanol, the culture supernatants, stored at −20°C, were thawed on ice, heated (80°C, 5 min), centrifuged (16,000 × *g*, 5 min, 4°C), and filtered (0.2-μm-pore-size cellulose filter). High-pressure liquid chromatography (HPLC; Merck-Hitachi HPLC System, model D-6000) was performed using a ICPSep Coregel 87H3 column (Transgenomic, Inc., Omaha, NE) and 0.005 M H_2SO_4 as the eluent. Organic acids were detected with UV-VIS detector (L-4250; Merck Hitachi) at 210 nm and ethanol with an RI-detector (Merck Hitachi) at 190 nm. The data analysis was performed by the D-7000 HPLC system manager software (version 3.1.1; Hitachi). Ammonium strips (Quantofix; Macherey-Nagel, Dueren, Germany) were used for monitoring ammonium ions.

Preparation of protein extracts. The cells (50 ml) were harvested from different growth phases by centrifugation (13,100 × *g*, 10 min, 4°C), washed twice with TE-PMSF (10 mM Tris, 1 mM EDTA, 14 μM phenylmethylsulfonyl fluoride [pH 7.5]), and resuspended in TE-PMSF buffer. For cell lysis, lysozyme (1 mg ml^{-1}, with incubation on ice for 1 h) was added, followed by sonication (Labsonic U; B. Brown Biotech International, Melsungen, Germany) with a 0.6 repeating duty cycle of 5 × 30 s with 1-min intervals. Cell debris was removed by centrifugation (20,000 × *g*, 2 × 30 min, 4°C). The supernatants were assayed for protein concentration with the RotiNanoquant kit (Roth, Karlsruhe, Germany) and adjusted to 360 μl with denaturation solution (2 M thiourea, 8 M urea) per 200 μg of protein. The samples were stored at −20°C if not immediately used.

2-DE. Protein samples from four independent cultivations were analyzed using the 2-DE method as described by Büttner et al. (8). In brief, the crude protein extract (360 μl in 2 M thiourea–8 M urea) was supplemented with 40 μl of CHAPS {3-[(3-cholamidopropyl)-dimethylammonio]-1-propanesulfonate} solution (20 mM dithiothreitol [DTT], 1% [wt/vol] CHAPS, 0.5% [vol/vol] Pharmalyte pH 3 to 10), loaded onto 3 to 10 range immobilized pH gradient (IPG) strips (Amersham Biosciences, Uppsala, Sweden), and incubated for 16 h at room temperature. The IEF was performed by use of a Multiphor II unit (Amersham biosciences), after which the strips were equilibrated with DTT and iodoacetamide solutions for 15 min as described by Görg et al. (22). The SDS-PAGE was performed with an Investigator 2-D electrophoresis system (Genomic Solutions, Chelmsford, MA) with 2 W per gel. The resulting 2-DE gels were fixed with 40% (vol/vol) ethanol in 10% (vol/vol) acetic acid for 2 h and subsequently stained with SYPRO Ruby (Bio-Rad, California) according to the manufacturer's instructions. Protein spots were visualized with Storm860 fluorescence imager (Amersham Pharmacia Biotech, Uppsala, Sweden). The proteins were identified by using matrix-assisted laser desorption ionization–time of flight (MALDI-TOF) and MALDI-TOF-TOF as reported by Liedert et al. (38).

Image analysis and statistics. The protein spot patterns were analyzed with the Delta2D software version 4.1 (Decodon GmbH, Germany). One-way analysis of variance (ANOVA) combined with permutation testing (1,000 permutations) was used to find significantly changed spots using confidence level of 95%. False significant number was limited to 10, i.e., 10 of 1,000 analyzed spots can be false positives.

RESULTS

Growth of *D. geothermalis* in low-carbon medium. *D. geothermalis* E50051 was cultivated in modified R2 broth containing 2.3 g of organic substrate per liter similar to paper machine water circuits (45). R2 broth, which is widely used in water microbiology (16), was modified by replacing glucose with starch. R2 favors biofilm growth of *D. geothermalis* in contrast to rich media. Figure

1 shows that during active growth ($\mu = 0.8\ h^{-1}$) oxygen was consumed, seen as a decrease of pO_2 in the medium. When the growth rate attenuated ($\mu = 0.06\ h^{-1}$), the concentration of dissolved oxygen in the medium increased, indicating that less oxygen was used than what entered into the medium by mixing. The accumulation of succinic acid in the medium was observed (Fig. 1). The initial rate of succinic acid production was 47 mg liter^{-1} h^{-1} ($\mu = 0.8\ h^{-1}$), then 28 mg liter^{-1} h^{-1} ($\mu = 0.06\ h^{-1}$), and then in the stationary phase 7 mg liter^{-1} h^{-1} ($\mu = 0.01\ h^{-1}$). No formic acid, ethanol, lactic, acetic, butyric, malic, propionic, or valeric acid was produced. Free ammonium ions were emitted to the medium (>10 mg liter^{-1}), indicating that peptides were used as a carbon source. Production of ammonia explains why pH did not fall below the initial value of 6.8 despite of extensive production of succinic acid (Fig. 1). A measurable consumption of starch by *D. geothermalis* was first observed 4 h postinoculation when the growth of *D. geothermalis* was slowing down (retention growth phase [Ret], Fig. 1), indicating that during exponential growth pyruvate or peptides were used as preferred substrates.

Functional proteomic analysis. 2-DE and bioinformatics tools were used to compare the cytosolic proteomes of *D. geothermalis* cells harvested in the exponential growth phase ($\mu = 0.8\ h^{-1}$, Exp in Fig. 1), early retardation phase ($\mu = 0.06\ h^{-1}$, Ret in Fig. 1), early stationary phase ($\mu = 0.02\ h^{-1}$, Stat1 in Fig. 1) and at the stationary phase (Stat2 and Stat3 in Fig. 1). SYPRO Ruby-stained 2-DE gels (dual-channel images are shown in Fig. 2) containing 1,021 spots, from which 403 were identified as described earlier (38). Statistical analysis with one-way ANOVA identified 165 protein spots whose expression ratios were changed during growth, displayed as a heat map in Fig. 3. From these, 47 protein spots had known identities (labeled in Fig. 3 and Fig. 2A with corresponding numbers), which were grouped into functional classes.

ATP production. The NADH dehydrogenase (Dgeo_1949, #36 [the "#number" designations refer to the protein numbers used in Fig. 2A and Fig. 3]) was downregulated in the stationary phase. The subunits of V-type ATPases (AtpB, #16; AtpD, #21) (Table 1) were found among the 40 most abundant proteins in growing cells but not in the stationary-phase cells. No F_1F_0 type ATPase is encoded by the genome of *D. geothermalis* (42). Attenuation of respiration at stationary phase can be seen as an increase of the dissolved oxygen in the medium (Fig. 1). *D. geothermalis* grew better on R2 agar plates cultivated in a low-oxygen atmosphere (1% O_2, 1% CO_2) compared to an ambient atmosphere (data not shown) but did not grow in the complete absence of O_2 and CO_2 even if alternative electron acceptors were added [MnO_2, Fe (III), nitrate, fumarate]. This indicates *D. geothermalis* is well adapted to low-oxygen conditions.

Combating oxidative stress. One of the key enzymes of oxidative defense, superoxide dismutase (manganese dependent SodA, #6) became the third most abundant protein in the stationary-phase proteome (Table 1) and remained abundant throughout monitored stationary phase (Fig. 3). The hydrogen peroxide-neutralizing enzyme, catalase (KatA, #27), was highly expressed in the early stationary phase. In the presence of ferrous ions, catalase generates reactive oxygen radicals when splitting the hydrogen peroxide into oxygen and water. The enzyme lysine 2,3-aminomutase (Dgeo_0988, #74, *S*-adenosylmethionine superfamily of enzymes) generates reactive radicals in the presence of a 4Fe-4S cluster and *S*-adenosylmethione. Both of these enzymes (#27 and #74) were downregulated in the late stationary phase (Fig. 3). This could be a part of the stress survival strategy of *D. geothermalis* under conditions where the environment was saturated with oxygen but the consumption of oxygen was low or none (Fig. 1).

Many enzymes involved in combating oxidative stress, including superoxide dismutase, require Mn for activity. We evaluated the role of manganese for the growth of *D. geothermalis* by adding $MnCl_2$ (100 μM) at the onset of the stationary growth phase into R2 starch broth medium which has $\leq$10 μg of soluble Mn liter^{-1}, a level similar to the levels in natural waters. Mn addition resulted in resumed oxygen consumption, a 40% increase in biomass density (OD_{600}) and transient acidification of the medium. It is interesting that the acidification of the medium and restart of oxygen consumption occurred in tandem (Fig. 1 and 4) and also reversed simultaneously (Fig. 4). These findings indicate that acid production and oxygen consumption were not alternative metabolic routes but parallel with each other.

Repair proteins. The three members of Suf Fe-S assembly protein system—SufB (Dgeo_0473, #32), SufC (Dgeo_0474, #52), and SufD (Dgeo_0472, #46)—were upregulated (Fig. 3) and were among the most abundant proteins in nongrowing cells but not in growing cells (Table 1). The protein repair enzyme, peptidylprolyl isomerase (Dgeo_0070, #61), and the chaperones GroEL (#2), DnaJ (#68), and Hsp20 (Dgeo_0505, #47) were induced in the stationary phase. Chaperones GroEL, DnaK, and GroES were found among the six most abundant proteins both in growing and in nongrowing cells (Table 1). Other upregulated enzymes with a possible role in stress response were the osmotically inducible protein OsmC (Dgeo_0526, #38) and the pyridoxine biosynthesis protein PdxS (#69).

Substrate level phosphorylation. The pentose phosphate pathway for glucose oxidation (PPP) was upregulated during transition to stationary phase, depicted by upregulation of the glucose-6-phosphate dehydrogenase (Dgeo_1974, #66) and 6-phosphogluconate dehydrogenase (Dgeo_1973, #67) as seen in Fig. 3. This pathway enables the complete conversion of glucose to CO_2 by producing glyceraldehyde-3-phosphate, 3 CO_2 and 6 $NADPH_2$. Glyceraldehyde 3-phosphate can be further converted to glycerate 3-P and ATP in the nonoxidative part of PPP by glyceraldehyde-3-P dehydrogenase (Dgeo_1133, #8), abundantly present in the cells in all growth stages (Table 1), and phosphoglycerate kinase (Pgk, #70). Pgk, the ATP-producing enzyme of the glycolytic pathway, was transiently upregulated when growth attenuated (Fig. 3).

Central carbon metabolism. When the growth slowed down, the ATP-producing glycolytic enzyme, pyruvate kinase (Dgeo_0005, #71), and the citric acid cycle enzyme, citrate synthase (GltA, #78), were downregulated (Fig. 3), suggesting that the cessation of growth turned off the citric acid cycle. As the oxidative pentose phosphate pathway was upregulated (glucose-6-phosphate dehydrogenase #66 and 6-phosphogluconate dehydrogenase #67; Fig. 3), a majority of the carbon (from starch) may have entered the central carbon metabolism via this pathway. Conversely, isocitrate dehydrogenase (Dgeo_1166, #64) was upregulated (Fig. 3). According to the bioinformatic portal UniprotKB (Protein Knowledgebase), only the NADP-dependent isozyme of isocitrate dehydrogenase is coded by the genome of *D. geothermalis*. Other citric acid cycle enzymes, fumarase C (FumC, #58) and malate dehydrogenase (Mdh, #72), appeared on the gel as double

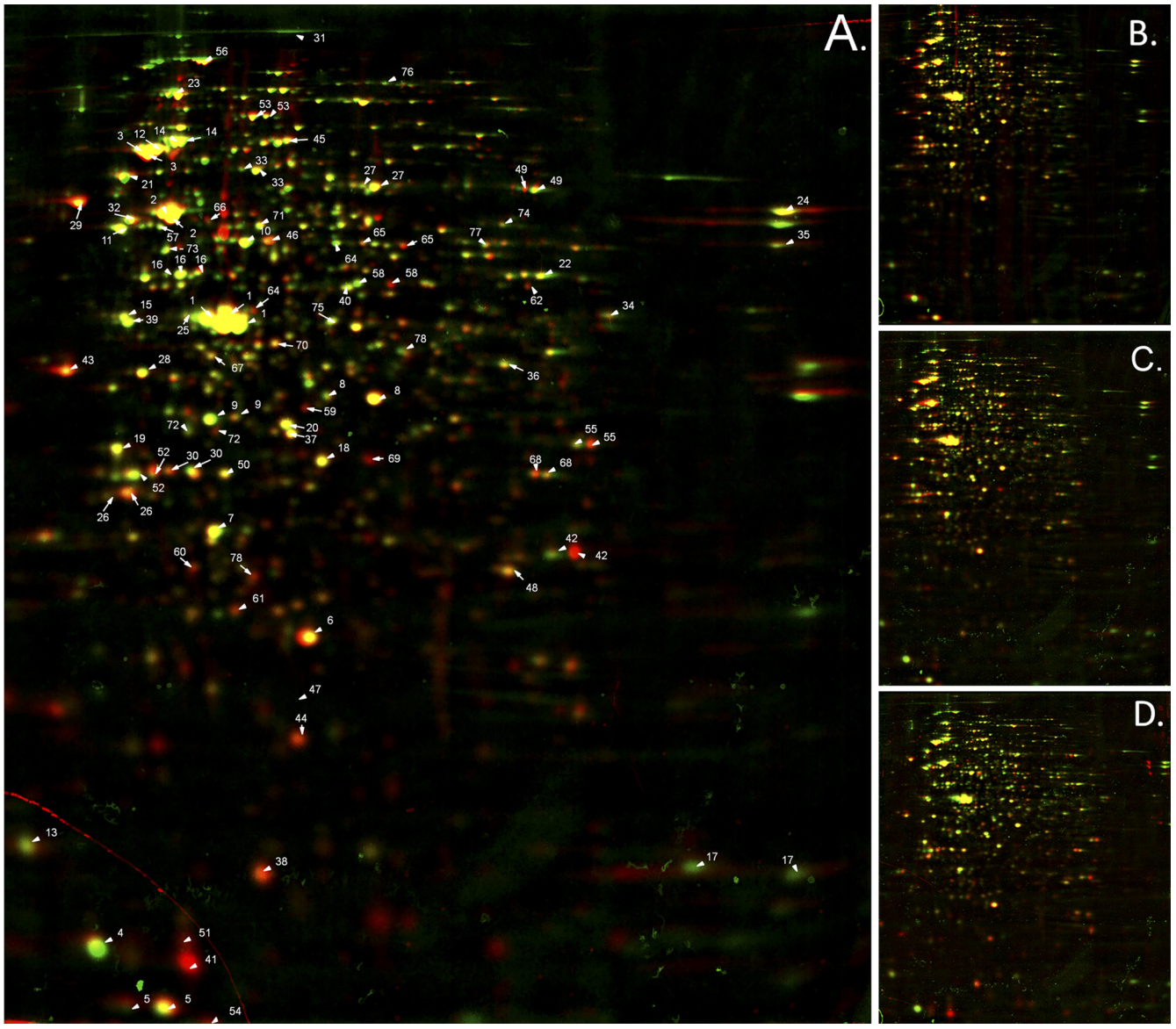

FIG 2 Dual 2-DE gel images showing the changes of protein expression by *D. geothermalis* during declining growth in liquid culture. *D. geothermalis* was grown aerobically in oligotrophic medium (R2 starch) at 45°C and harvested during exponential growth ($\mu = 0.8\ h^{-1}$) and declining growth ($\mu = 0.6$ down to $\leq 0.01\ h^{-1}$, see Fig. 1). Protein expression patterns were analyzed using 2-DE and bioinformatics tools. The resulting gel from the exponential growth phase ($\mu = 0.8\ h^{-1}$, "Exp" in Fig. 1) was artificially stained red with image analysis software and is overlaid in the dual view with those of the declining growth phases (shown in Fig. 1): $\mu \leq 0.01\ h^{-1}$ ("Stat2") (A), $\mu = 0.06\ h^{-1}$ ("Ret") (B), $\mu = 0.02\ h^{-1}$ ("Stat1") (C), and $\mu =$ not detected ("Stat") stained green (D). Spots with identical expression appear in yellow. The most abundant proteins (Table 1) in exponentially growing ("Exp") and/or in nongrowing cells ("Stat2") and the proteins with significant expression changes (shown in Fig. 3) are labeled in panel A. The gels were SYPRO Ruby stained.

spots that showed opposite expression patterns (Fig. 2A), possibly representing modified protein isoforms. Together, these findings imply that the citric acid cycle was segmented to upregulated and downregulated parts and was not used for channeling pyruvate to CO_2 and NADH required for respiration. Instead, the carbon metabolism in nongrowing cells was likely aimed for the production of NADPH.

Proteins with unknown function. Three proteins with no homology to proteins with a known function were induced (Fig. 3). Dgeo_0571 (#41) became highly abundant in stationary-phase cells (Table 1). BLAST search showed that the protein belongs to an amino acid kinase superfamily. Dgeo_0275 (#51) and Dgeo_1454 (#43) had no conserved domains, and thus no putative function can be given for them.

Nitrogen metabolism. Three enzymes of the arginase pathway—arginase (Dgeo_0292, #30), ornithine aminotransferase (ArgD, #34), and 1-pyrroline-5-carboxylate dehydrogenase (Dgeo_0850, #57)—were transiently upregulated in the nongrowing cells (Fig. 3). These enzymes are reversible, metabolizing either glutamate to arginine or vice versa. Since glutamate is an abundant amino acid residue in R2, it is likely that glutamate was metabolized into ornithine-producing 2-oxoglutarate, a reaction catalyzed by ornithine aminotransferase.

Cell growth and proliferation. Translation proteins, includ-

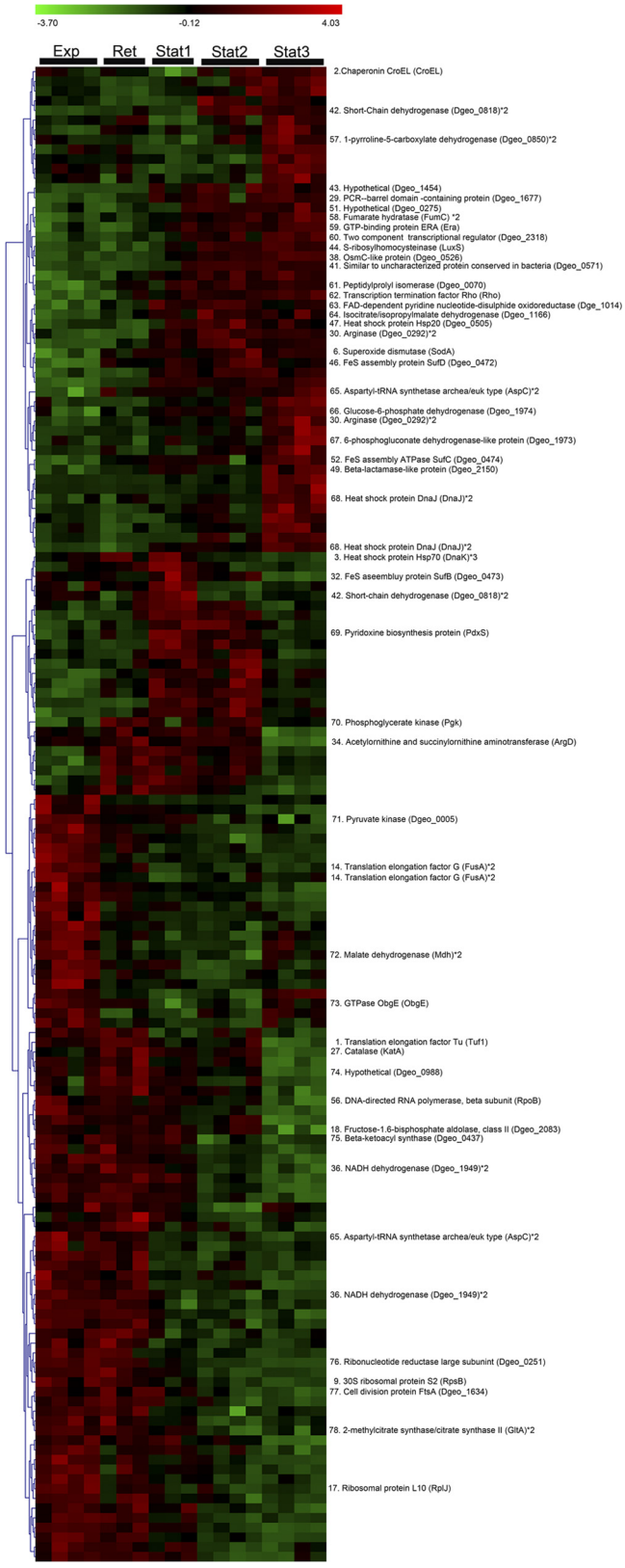

FIG 3 Heat map for the significantly changed proteins of *D. geothermalis* E50051 proteomes prepared from cells harvested at the exponential (Exp), retardation (Ret), and stationary (Stat1, Stat2, and Stat3) phases as displayed in Fig. 1. SYPRO Ruby-stained 2-DE gels were prepared from three or four independent cultivations and quantitatively analyzed by one-way ANOVA and permutation tests. Hierarchical clustering was done by using complete linkage and Pearson correlation of expression profiles. A total of 47 spots had known identities (Liedert et al. [38]).

ing elongation factor Tu (Tuf1, #1), ribosomal protein L10 (RplJ, #17), translation elongation factor G (FusA, #14), and aspartyl-tRNA synthetase (AspC, #65) as well as transcription protein DNA-directed RNA polymerase (RpoB, # 56) and cell division protein FtsA (#77), were downregulated in nongrowing cells (Fig. 3). A reduced synthesis rate was also seen in the upregulation of the transcription termination factor Rho (#62). Translation-related proteins include several highly abundant proteins (Table 1), tRNA synthetases, and ribosomal proteins, which appeared typically in double spots. The MS data did not reveal whether these were posttranslational modifications or artifacts due to sample treatment.

Signaling and regulation proteins. Four proteins with putative regulatory function were induced in stationary-phase cells, namely, *S*-ribosylhomocysteinase (LuxS, #44), the two-component transcriptional regulator (Dgeo_2318, #60) belonging to the OmpR family, and the GTPases Era (#59) and ObgE (#73). These GTPases showed opposite expression patterns so that ObgE was downregulated while Era was upregulated.

DISCUSSION

The natural habitats of *D. geothermalis* are geothermal springs (17) and hydrothermal vents in deep-ocean subsurfaces (34). In the present study, we used proteomic tools to understand how this bacterium may adapt to life on aerobic, warm industrial waters. The bacterium was cultivated aerobically in a medium containing no redox-negative substances such as glucose or Mn ions beyond those that may occur in natural waters. The observed proteomic changes indicated that the growth-arrested cells ($\mu < 0.06\ h^{-1}$) compared to the growing cells ($\mu = 0.8$) suffered from oxidative stress, seen as the downregulation of oxygen-consuming reactions, oxidative phosphorylation, and of glycolysis, and upregulation of protective enzymes and pathways discussed in detail below. Reactive by-products from oxygen are generated continuously in the metabolism and are a major threat for aerobically growing cells (9, 29). Defenses against an internal oxidative threat are essential for a nongrowing cell (15) since considerable ROS production continues in the stationary phase (20).

Role of succinate in combating ROS. As a novel finding for the genus *Deinococcus*, we showed extensive conversion of organic substrates into succinic acid during active growth when oxygen consumption was highest (Fig. 1), whereas no other carboxylic acid or ethanol was produced. Thus, the results indicate that succinic acid production was not a fermentative process. Combining the proteome data and bioinformatics tools, we suggest five pathways that may be responsible for the production of succinic acid (summarized in Fig. 5). First, the products of upregulated isocitrate dehydrogenase are 2-oxoglutarate, NADPH, and CO_2. 2-Oxoglutarate is an essential component in combating ROS and known to spontaneously react with ROS, yielding succinic acid as the product (41). Second, 2-oxoglutarate could be supplied by the turnover of amino acids (Pro, Glu, and Arg) retrieved from the growth medium (yeast extract and peptones) and be further catabolized into NADPH and succinic acid. Third, succinic acid may

TABLE 1 The 40 most abundant proteins of the soluble fraction of *D. geothermalis* E50051 during the exponential ($\mu = 0.8\ h^{-1}$) and ceasing ($\mu < 0.02\ h^{-1}$) phases of growth

Protein[a]	%V[b]	Identity[c]	Protein[a]	%V[b]	Identity[c]
Exponential phase (Exp)			Stationary phase (Stat2)		
Elongation factor Tu (Tuf1) *3	2.93	1	Elongation factor Tu (tuf1) *3	3.75	1
Chaperonin GroEL (GroEL)*2	2.37	2	Chaperonin GroEL (GroEL)*2	2.65	2
Heat shock protein Hsp70 (DnaK) *2	1.35	3	Mn-superoxide dismutase (SodA)	1.58	6
Ribosomal protein L7/L12 (RplL)	1.28	4	Hypothetical protein (Dgeo_0571)	1.45	41
Co-chaperonin GroES (GroES) *2	0.93	5	Heat shock protein Hsp70 (DnaK) *2	1.42	3
Mn-superoxide dismutase (SodA)	0.88	6	Co-chaperonin GroES (GroES) *2	1.24	5
Elongation factor Ts (Tsf)	0.86	7	Glyceraldehyde-3-phosphate dehydrogenase (Dgeo_1133) *2	1.06	8
Glyceraldehyde-3-phosphate dehydrogenase (Dgeo_1133) *2	0.78	8	OsmC (Dgeo_0526)	1.00	38
30S ribosomal protein S2 (RpsB) *2	0.74	9	PRC-barrel domain-containing protein (Dgeo_1677)	0.85	29
Thermostable carboxypeptidase 1 (Dgeo_0334)	0.73	10	Elongation factor Ts (Tsf)	0.84	7
Trigger factor (Tig)	0.72	11	Ferritin and Dps (Dps) *2	0.68	26
30S ribosomal protein S1 (Dgeo_1577)	0.68	12	Short-chain dehydrogenase (Dgeo_0818) *2	0.66	42
Hypothetical protein (Dgeo_1085)	0.66	13	Fructose-1,6-bisphosphate aldolase (Dgeo_2083)	0.64	18
Translation elongation factor G (FusA) *2	0.63	14	Hypothetical protein (Dgeo_1454) *2	0.62	43
DNA-directed RNA polymerase, alpha subunit (RpoA)	0.61	15	Thermostable carboxypeptidase 1 (Dgeo_0334)	0.61	10
V-type ATPase subunit B (AtpB) *3	0.58	16	Arginase (Dgeo_0292) *2	0.61	30
Ribosomal protein L10 (RplJ)	0.56	17	*S*-Ribosylhomocysteinase (LuxS)	0.60	44
Fructose-1,6-bisphosphate aldolase (Dgeo_2083)	0.56	18	Glutamine synthetase (Dgeo_1203)	0.60	45
50S ribosomal protein L25 (RplY)	0.55	19	FeS assembly protein SufD (Dgeo_0472)	0.59	46
Single-strand binding protein (Ssb)	0.52	20	Single-strand binding protein (Ssb)	0.57	20
V-type ATPase, D subunit (AtpD) *2	0.50	21	2-oxoglutarate dehydrogenase, E2 component (Dgeo_1682) *2	0.55	23
Dihydrolipoamide dehydrogenase (Dgeo_0353) *2/4-aminobutyrate aminotransferase (Dgeo_0989)	(0.50)	22	Catalase (KatA) *2	0.54	27
2-oxoglutarate dehydrogenase, E2 component (Dgeo_1682) *2	0.49	23	Heat shock protein Hsp20 (Dgeo_0505)	0.53	47
Extracellular solute-binding protein (Dgeo_1344)	0.49	24	Short-chain dehydrogenase (Dgeo_0260)	0.52	48
Aminotransferase (Dgeo_2084)	0.46	25	Bacterial extracellular solute-binding protein (Dgeo_1189)	0.52	35
Ferritin and Dps (Dps) *2	0.45	26	Trigger factor (Tig)	0.36	11
Catalase (KatA) *2	0.45	27	Beta-lactamase-like protein (Dgeo_2150) *3	0.48	49
Cell division protein FtsZ (Dgeo_1635)	0.44	28	Hypothetical protein (Dgeo_1085)	0.47	13
PRC-barrel domain-containing protein (Dgeo_1677)	0.43	29	30S ribosomal protein S2 (RpsB) *2	0.46	9
Arginase (Dgeo_0292) *2	0.39	30	FeS assembly protein SufB (Dgeo_0473) *2	0.45	32
DNA-directed RNA polymerase, beta subunit (rpoB) *2	0.39	31	Nitrilase (Dgeo_0036)/electron transfer flavoprotein (Dgeo_0720) *2	(0.44)	50
FeS assembly protein SufB (Dgeo_0473) *2	0.39	32	Hypothetical protein (Dgeo_0275)	0.44	51
Bacterial transketolase (Dgeo_2283) *2	0.38	33	FeS assembly ATPase SufC (Dgeo_0474) *2	0.44	52
Acetylornithine and succinylornithine aminotransferase (ArgD)	0.38	34	DNA-directed RNA polymerase, alpha subunit (RpoA)	0.43	15
Bacterial extracellular solute-binding protein (Dgeo_1189)	0.38	35	ATPase AAA-2 (ClpB) *4	0.43	3
NADH dehydrogenase (Dgeo_1949) *2	0.38	36	Hypothetical protein (Dgeo_1167)	0.43	54
3-hydroxyacyl-CoA dehydrogenase (Dgeo_0379)	0.37	37	Extracellular solute-binding protein (Dgeo_1344)	0.42	24
OsmC (Dgeo_0526)	0.37	38	Translation elongation factor G (FusA) *2	0.42	14
Enolase (Eno)	0.35	39	Dihydrolipoamide dehydrogenase (Dgeo_0353) *2/4-aminobutyrate Aminotransferase (Dgeo_0989)	(0.40)	22
S-Adenosylmethionine synthetase (MetK)	0.35	40	CRISPR-associated protein Csd2 family protein (Dgeo_0236) *3	0.40	55

[a] The spots are marked in the 2-DE image in Fig. 2A. Digits with asterisks (*2, etc.) indicate the respective numbers of spots (i.e., protein isoforms) on the 2-DE gel at pI range 3 to 10.

[b] %V, relative quantity of the spot, excluding the background. The total quantity of all spots on the gel is 100%.

[c] That is, the protein code in the 2-DE gel (Fig. 2A).

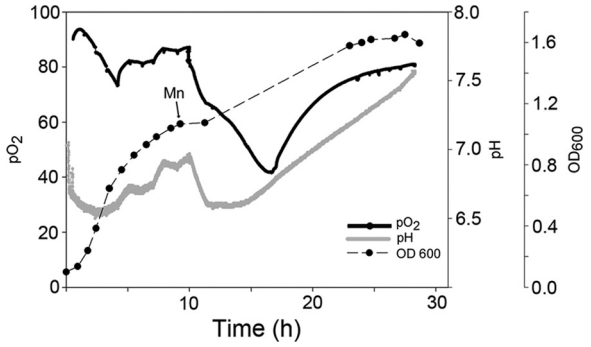

FIG 4 Effect of manganese (100 μM $MnCl_2$) addition on the growth parameters of *D. geothermalis* E50051 grown aerobically at 45°C in R2 starch broth. The pH and the concentration of dissolved oxygen were monitored online. Aeration was administered by constant agitation throughout the cultivation.

come from the cleavage of isocitrate via the glyoxylate shunt. Its key enzymes, isocitrate lyase (Dgeo_1287) and malate synthase (Dgeo_2616), were not identified in the proteome, but their genes have been found in the *D. geothermalis* genome. This pathway was reported to become upregulated in *D. radiodurans* cells recovering from radiation stress (40). As a fourth option which does not serve ROS detoxification, succinic acid could be produced from pyruvate via anticlockwise operation of tricarboxylic acid (TCA) cycle as the isoforms of malate dehydrogenase and fumarate hydratase were upregulated (Fig. 2A and Fig. 3, #63 and #70). These enzymes had isoforms on the 2-DE gels, making it difficult to confirm this possibility. A fifth option for the succinate production could be the conversion of 2-oxoglutarate via succinyl-CoA to succinate, but no expression change was observed for oxoglutarate dehydrogenase or succinyl CoA synthase. We anticipate more detailed studies to determine which of the pathways are active in *D. geothermalis* cells converting a large part of the medium contained carbon into succinate.

Cost of manganese limitation. The addition of manganese (100 μM, i.e., 5,500 μg liter^{-1}) to the culture, which had already ceased to grow, induced new round of cell division, reinitiated the respiration of the *D. geothermalis* cells, and simultaneously caused the acidification of the medium (Fig. 4). Thus, we propose that the production of succinate from organic substrates was the price caused by the need of combating respiration derived ROS under manganese limitation (10 μg liter^{-1}). Manganese-induced cell division (Mn-CD) was also observed in *D. radiodurans* in a glucose-containing rich medium (11, 61). An Mn supplement was shown to be essential for high-cell-density cultivation of *D. radiodurans* (24). The high intracellular concentrations of manganese and low levels of iron ions have been suggested to protect proteins of *D. radiodurans* from reactive oxygen species (ROS) and their oxidative effects, thus allowing the repair enzymes to function and repair cellular damage caused by desiccation and irradiation (12, 18, 19). Also, *D. geothermalis* was shown to accumulate manganese (12). Mn(II) ions can scavenge $O_2^{\cdot -}$ (2) and protect proteins from oxidative modifications (13) and also are cofactors in essential enzymes, such as SODs and catalases (reviewed in reference 30).

Carbon metabolism aims at production of NADPH. During the retardation phase the cells downregulated glycolytic enzymes, leading to the citric acid cycle, and upregulated the oxidative PPP- and NADPH-producing enzyme, isocitrate dehydrogenase (illustrated in Fig. 5). The genome of *D. geothermalis* does not appear to encode for an NADH-dependent isocitrate dehydrogenase. The NADP-dependent forms of Icd and other NADPH-generating isozymes were also shown to be upregulated in *Pseudomonas fluorescens* under oxidative stress (52). In addition, we observed the upregulation of a putative NADP-ferredoxin reductase FprA (Dgeo_1014) which has been suggested to modulate the NADPH homeostasis (36) and to serve as a defense barrier against oxidative damage in *Escherichia coli* (4). We conclude that central carbon metabolism in *D. geothermalis* cells suffering from oxidative stress was rechanneled to pathways where mainly NADPH, and not NADH, was retrieved from the carbon substrate. This may be in part because the effectiveness of SodA, KatA, and thioredoxin as scavengers of ROS is dependent on the availability of NADPH. It is also possible that in *D. geothermalis* the TCA cycle does not function as a cycle aimed at the production of NADH to feed oxidative phosphorylation at any growth rate, thus evading the intracellular oxidative damage generated when NADH is aerobically metabolized. Earlier studies show that metabolites generated by PPP from glucose increase the survival of *D. radiodurans* (61). Further, the presented data are congruent with those of Zhang et al. (61), who reported that TGY-grown *D. radiodurans* metabolized glucose solely by PPP.

Battle against oxidative damage. The battle against oxidative damage was seen as the upregulation of the two key enzymes: superoxide dismutase and catalase (Fig. 3). Of the most abundant proteins in nongrowing cells, 18% (7/40) were protein repair enzymes compared to only 10% (4/40) in growing cells (Table 1). GroEL, DnaK, and GroES were abundant throughout the growth. Chaperones assist the proper *de novo* folding of proteins under normal conditions, restore the activity of conformationally damaged proteins, and function in proteolysis (21, 23). Chaperones Hsp20 (Dgeo_0505) and DnaJ were upregulated when the cells entered the stationary phase. The observed changes are similar to the proteome of heat-stressed *D. radiodurans*, showing that GroEL, DnaK, Hsp20, SodA, and protease PfpI (similar to Dgeo_0863) were induced (1). DnaK, GroES, PspA, Hsp20, and DR1314 (similar to upregulated hypothetical protein Dgeo_1454, Fig. 3) of *D. radiodurans* are regulated by heat shock regulator Sig1 (51). Sig1 is one of the only three sigma factors encoded by the genome of *D. radiodurans*. Similarities between the proteomic signatures observed in the present study and the previous heat shock studies with *D. radiodurans* suggest that the oxidative stress response connected to the growth arrest is also regulated by Sig1 in *D. geothermalis*. Chaperones and proteins belonging to either oxidative or heat stress stimulons have been shown to be induced in starving cells. This may provide the cells with cross-protection against various stressors that cells may encounter in their natural environments (31, 15).

Three members of the Suf assembly family that were induced in nongrowing cells of *D. geothermalis* are known to be responsible for ATP-coupled assembling and repairing proteins with exposed $[Fe\text{-}S]_x$ clusters under oxidative stress (43). Fe-S clusters are very sensitive to inactivation by ROS but are nevertheless the most abundant and diversely employed enzymatic cofactor (29). In resistant bacteria, the unstable Fe-S enzymes are replaced by more resistant isozymes (reviewed in references 19 and 28). *D. geothermalis* expressed only one fumarase belonging to class II, similar to the resistant, iron-independent isozyme fumarase C of *E. coli* expressed under oxidative attack (39). In this respect, *D. geotherma-*

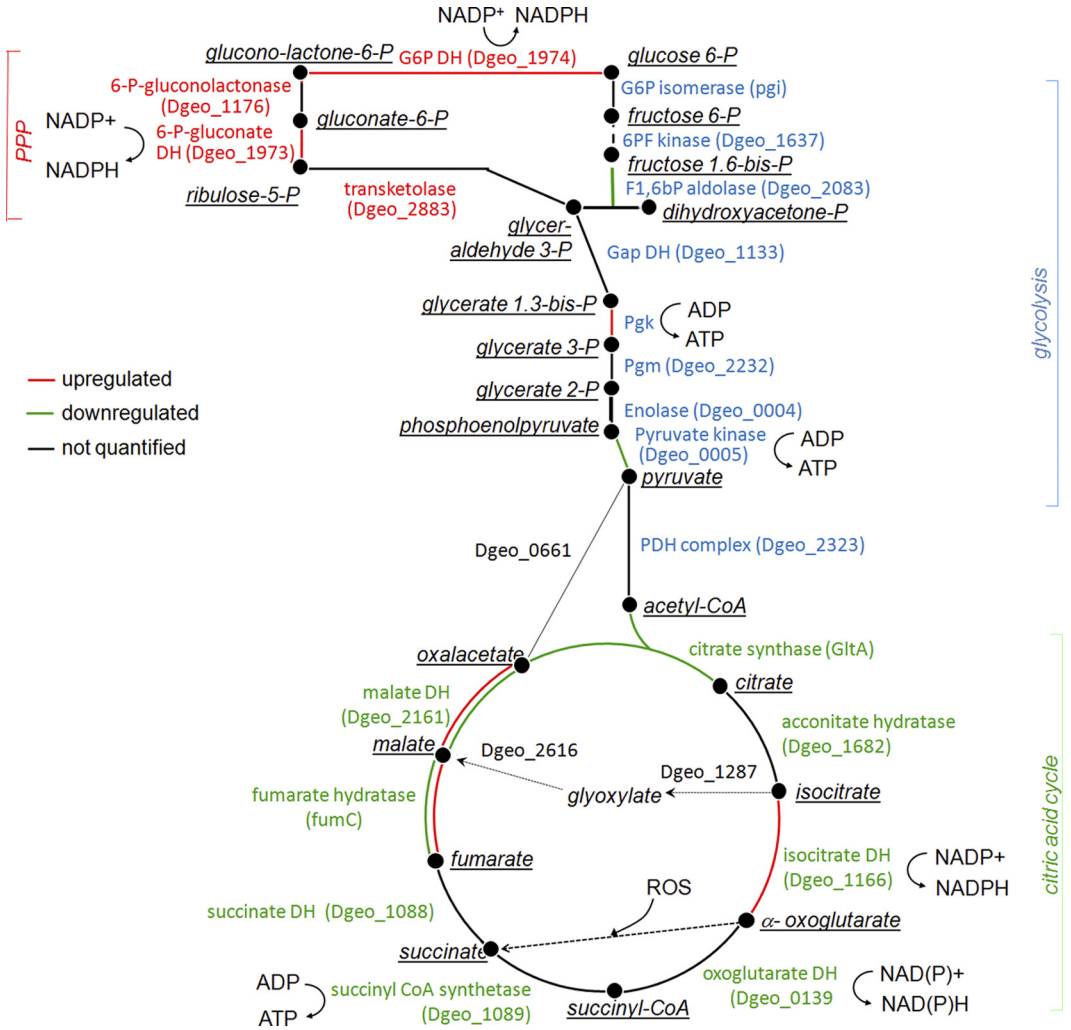

FIG 5 Metabolic scheme for the main routes of carbon flow of *D. geothermalis* E50051 during active growth and nongrowth. The steps are color coded to illustrate enzyme expression change in nongrowing cells compared to growing cells. Red lines indicate upregulated enzymes in stationary-phase cells, and green lines indicate downregulated enzymes. When an enzymes appeared in double spots on the gel and the expression of the spots were different, the two lines are marked with corresponding colors. When no common protein name was available in the databases, the gene locus code is given (in parentheses).

lis is similar to mammals that also have only cluster-free fumarase. Another induced protein repair enzyme was peptidylprolyl isomerase (Dgeo_0070), which can reverse a covalent damage to proline (56). These results show that protein maintenance and repair represented the main metabolic activities of the nongrowing cells with limited synthesis capacity. Protection from protein oxidation has been implicated as a primary determinant of radioresistance of *D. radiodurans* (13).

The osmotically inducible protein OsmC whose homologue (Dgeo_0526, #38) was upregulated in *D. geothermalis* is involved in the defense against oxidative stress caused by exposure to organic hydroperoxides produced during aerobic respiration in bacteria (37). The present study shows the upregulation also of pyridoxine biosynthesis protein PdxS (#69), which is involved in the synthesis of vitamin B_6, an efficient singlet oxygen quencher and a potential antioxidant (5).

Aerobic ATP production. Transition from growth to nongrowth resulted, as expected, in decreased oxidative phosphorylation, seen as a downregulation of the V-type ATPases responsible for ATP synthesis in *D. geothermalis* and as a rise in the level of dissolved oxygen in the medium (Fig. 2). Prokaryotic or archaeal type V-type ATPases have been reported to produce ATP driven by the proton gradient in *Thermus thermophilus* (54, 60). *D. geothermalis* upregulated the PPP cycle to provide cells with ATP and NADPH. *D. geothermalis* was described as a strict aerobe (17). Anaerobic reduction of Cr(IV) by *D. geothermalis* has been reported (7), but there is no indication of its connection to ATP production. We observed that *D. geothermalis* grew well in a low-oxygen atmosphere (1% O_2, 1% CO_2), even better than under an air influx. The genome of *D. geothermalis* codes for a putative nitrite reductase and a formate dehydrogenase (42), but these typical membrane proteins were not detectable in the cytoplasmic proteome. The membrane proteome of *D. geothermalis* grown in atmospheric air contained *d*- and *bd*-type cytochromes (53), which represent the high-affinity oxidases known to be expressed in a low-oxygen environment in *E. coli* (27, 32). We propose that the electron transport chain of *D. geothermalis* is adapted to a low-oxygen lifestyle, even when it grows in atmospheric air. This

may aid its survival in heterogenous biofilms where the local mass transfer coefficient for oxygen is very low (47). Preference of *D. geothermalis* for a low-oxygen environment could reflect the evolutionary origin of *Deinococcus* being on earth prior to the emergence of cyanobacteria (21) and the appearance of oxygen in the atmosphere.

The nongrowing cells induced *S*-ribosylhomocysteinase (LuxS). LuxS is an autoinducer-2-producing protein involved in bacterial communication, regulating several phenotypic traits such as pathogenesis and biofilm formation (57). Quorum sensing has been shown to be involved in biofilm formation of *Pseudomonas aeruginosa* (14, 59). Induced also was a two-component transcriptional regulator (Dgeo_2318, #60) of the OmpR family known to be involved in a network regulating the initial adhesion and biofilm formation of *E. coli* (46). Induction of these signaling related proteins may thus contribute to the attachment and biofilm formation of *D. geothermalis* observed during the cultivation. *D. geothermalis* E50051 forms persistent biofilms on nonliving substrata in the R2 starch broth (48, 49) used in the present study. The GTP binding proteins, Era and ObgE, are involved in cell proliferation, development, signal transduction, and protein synthesis (6). ObgE was shown to be involved in ribosome maturation (50) and, as ribosomal proteins were downregulated (Fig. 3), the need for ObgE may have been diminished as well. The Era-like gene of *Listeria monocytogenes* is required for bacterial adhesion to nonliving surfaces (3) and could similarly regulate the attachment of *D. geothermalis*.

In conclusion, the proteome data and the direct physiological measurements suggest that aerobically cultivated *D. geothermalis* cells suffered from oxidative stress, a response that may have been enhanced by the lack of manganese. The energy of the nongrowing cells was directed to NADPH production required by the detoxification and repair enzymes, while the ROS-producing pathways, oxidative phosphorylation and glycolysis, were downregulated. Succinic acid was likely a product of the defense enzymes since it accumulated in the medium mainly during active respiration. We propose that *D. geothermalis* prefers to combat ROS using manganese-dependent ways but, when manganese is not available, central carbon metabolism is used to produce ROS-neutralizing carbon metabolites at the expense of a high utilization of energy substrate. These results may be applied in the development of *D. geothermalis* for biotechnological application such as modulation of the species for intermediate succinate production in a low-manganese medium.

ACKNOWLEDGMENTS

This study was supported by the Biofouling Project of the PINTA program of the Finnish Funding Agency for Technology and Innovation (TEKES). Further support from the Finnish Graduate School in Environmental Science and Technology (EnSTe [C.L.]) and the CoE "Photobiomics" of the Academy of Finland (grant 118637[M.P. and M.S.S]) is acknowledged.

We thank Mikael Niemistö for starch analysis.

REFERENCES

1. **Airo A, Chan SL, Martinez Z, Platt MO, Trent JD.** 2004. Heat shock and cold shock in *Deinococcus radiodurans.* Cell. Biochem. Biophys. **40**:277–288.
2. **Archibald FS, Fridovich I.** 1982. The scavenging of superoxide radical by manganeous complexes: *in vitro*. Arch. Biochem. Biophys. **214**:452–463.
3. **Auvray F, Chassaing D, Duprat C, Carpentier B.** 2007. The *Listeria monocytogenes* homolog of the *Escherichia coli* era gene is involved in adhesion to inert surfaces. Appl. Environ. Microbiol. **73**:7789–7792.
4. **Bianchi V, Haggård-Ljungquist E, Pontis E, Reichard P.** 1995. Interruption of the ferredoxin(flavodoxin) $NADP^+$ oxidoreductase gene of *Escherichia coli* does not affect anaerobic growth but increases sensitivity to paraquat. J. Bacteriol. **177**:4528–4531.
5. **Bilski P, Li MY, Ehrenshaft M, Daub ME, Chignell CF.** 2000. Vitamin B_6 (pyridoxine) and its derivatives are efficient singlet oxygen quenchers and potential fungal antioxidants. Photochem. Photobiol. **71**:129–134.
6. **Bourne HR, Sanders DA, McCormick F.** 1991. The GTPase superfamily: conserved structure and molecular mechanism. Nature **349**:117–127.
7. **Brim H, Venkateswaran A, Kostandarithes HM, Fredrickson JK, Daly MJ.** 2003. Engineering *Deinococcus geothermalis* for bioremediation of high-temperature radioactive waste environments. Appl. Environ. Microbiol. **69**:4575–4582.
8. **Büttner K, et al.** 2001. A comprehensive two-dimensional map of cytosolic proteins of *Bacillus subtilis.* Electrophoresis **22**:2908–2935.
9. **Cabiscol E, Tamarit J, Ros J.** 1999. Oxidative stress in bacteria and protein damage by reactive oxygen species. Int. Microbiol. **3**:3–8.
10. **Cash P.** 1998. Characterization of bacterial proteomes by two-dimensional electrophoresis. Anal. Chim. Acta **372**:121–145.
11. **Chou FI, Tan ST.** 1990. Manganese(II) induces cell division and increases in superoxide dismutase and catalase activities in an aging deinococcal culture. J. Bacteriol. **172**:2029–2035.
12. **Daly MJ, et al.** 2004. Accumulation of Mn(II) in *Deinococcus radiodurans* facilitates gamma-radiation resistance. Science **306**:1025–1028.
13. **Daly MJ, et al.** 2007. Protein oxidation implicated as the primary determinant of bacterial radioresistance. PLoS Biol. **5**:e92.
14. **Davies DG, et al.** 1998. The involvement of cell-to-cell signals in the development of a bacterial biofilm. Science **280**:295–298.
15. **Dukan S, Nyström T.** 1998. Bacterial senescence: stasis results in increased and differential oxidation of cytoplasmic proteins leading to developmental induction of the heat shock regulon. Genes Dev. **12**:3431–3441.
16. **Eaton AD, Clesceri LS, Rice EW, Greenberg AE.** 2005. Standard methods for the examination of water and waster water, 21st ed, p 9–35. APHA, Washington, DC.
17. **Ferreira AC, et al.** 1997. *Deinococcus geothermalis* sp. nov. and *Deinococcus murrayi* sp. nov., two extremely radiation-resistant and slightly thermophilic species from hot springs. Int. J. Syst. Bacteriol. **47**:939–947.
18. **Fredrickson JK, et al.** 2008. Protein Oxidation: key to bacterial desiccation resistance? ISME J. **2**:393–403.
19. **Ghosal D, et al.** 2005. How radiation kills cells: survival of *Deinococcus radiodurans* and *Shewanella oneidensis* under oxidative stress. FEMS Microbiol. Rev. **29**:361–475.
20. **Gonzáles-Flecha B, Demple B.** 1995. Metabolic sources of hydrogen peroxide in aerobically growing *Escherichia coli.* J. Biol. Chem. **270**:13681–13687.
21. **Gupta RS.** 1998. Protein phylogenies and signature sequences: a reappraisal of evolutionary relationships among archaebacteria, eubacteria, and eukaryotes. Microbiol. Mol. Biol. Rev. **62**:1435–1491.
22. **Görg A, Boguth G, Obermeier C, Posch A, Weiss W.** 1995. Two-dimensional polyacrylamide gel electrophoresis with immobilized pH gradients in the first dimension (IPG-Dalt): the state of the art and the controversy of vertical versus horizontal systems. Electrophoresis **16**: 1079–1086.
23. **Hayes SA, Dice JF.** 1996. Roles of molecular chaperones in protein degradation. J. Cell Biol. **132**:255–258.
24. **He Y.** 2009. High cell density production of *Deinococcus radiodurans* under optimized conditions. J. Ind. Microbiol. Biotechnol. **36**:539–546.
25. **Hecker M, Müllner S.** 2003. Proteomics of microorganisms: fundamental aspects and application, p 27–140. *In* Scheper T (ed), Advances in biochemical engineering biotechnology. Springer-Verlag, Berlin, Germany.
26. **Hecker M, Völker U.** 2004. Towards a comprehensive understanding of *Bacillus subtilis* cell physiology by physiological proteomics. Proteomics **4**:3727–3750.
27. **Hill S, Viollet S, Smith AT, Anthony C.** 1990. Roles for enteric d-type cytochrome oxidase in N_2 fixation and microaerobiosis. J. Bacteriol. **4**:2071–2078.
28. **Imlay JA.** 2006. Iron-sulfur clusters and the problem with oxygen. Mol. Microbiol. **59**:1073–1082.
29. **Imlay JA.** 2008. Cellular defenses against superoxide and hydrogen peroxide. Annu. Rev. Biochem. **77**:755–776.
30. **Jakubovich NS, Jenkinson HF.** 2001. Out of iron age: new insights into

the critical role of manganese homeostasis in bacteria. Microbiol. **147**: 1709–1718.
31. **Jenkins DE, Schultz JE, Matin A.** 1988. Starvation-induced cross protection against heat or H_2O_2 challenge in *Escherichia coli*. J. Bacteriol. **170**: 3910–3914.
32. **Jünemann S.** 1997. Cytochrome *bd* terminal oxidase. Biochim. Biophys. Acta **1321**:107–127.
33. **Kanto Oqvist C, et al.** 2008. Prokaryotic microbiota of recycled paper mills with low or zero effluent. J. Ind. Microbiol. Biotechnol. **35**:1165–1173.
34. **Kimura H, Asada R, Masta A, Naganuma T.** 2003. Distribution of microorganisms in the subsurface of the manus basin hydrothermal vent field in Papua New Guinea. Appl. Environ. Microbiol. **69**:644–648.
35. **Kolari M, Nuutinen J, Rainey FA, Salkinoja-Salonen MS.** 2003. Colored moderately thermophilic bacteria in paper-machine biofilms. J. Ind. Microbiol. Biotechnol. **30**:225–238.
36. **Krapp AR, et al.** 2002. The flavoenzyme ferredoxin (flavodoxin)-NADP(H) Reductase modulates NADP(H) homeostasis during the *soxRS* response of *Escherichia coli*. J. Bacteriol. **184**:1474–1480.
37. **Lesniak J, Barton WA, Nikolov DB.** 2003. Structural and functional features of the *Escherichia coli* hydroperoxide resistance protein OsmC. Protein Sci. **12**:2838–2843.
38. **Liedert C, et al.** 2010. Two-dimensional proteome reference map for the radiation resistant bacterium *Deinococcus geothermalis*. Proteomics **10**: 1–9.
39. **Liochev SI, Fridovich I.** 1992. Fumarase C, the stable fumarase of *Escherichia coli*, is controlled by the *soxRS* regulon. Proc. Natl. Acad. Sci. U. S. A. **89**:5892–5896.
40. **Liu Y, et al.** 2003. Transcriptome dynamics of *Deinococcus radiodurans* recovering from ionizing radiation. Proc. Natl. Acad. Sci. U. S. A. **100**: 4191–4196.
41. **Mailloux RJ, et al.** 2007. The tricarboxylic acid cycle, an Ancient metabolic network with a novel twist. PLoS One **2**:e690.
42. **Makarova KS, et al.** 2007. *Deinococcus geothermalis*: the pool of extreme radiation resistance genes shrinks. PLoS One **2**:e955.
43. **Nachin L, Loiseau L, Expert D, Barras F.** 2003. SufC: an unorthodox cytoplasmic ABC/ATPase required for [Fe-S] biogenesis under oxidative stress. EMBO **22**:427–437.
44. **Peltola M, et al.** 2008. Quantitative contributions of bacteria and of *Deinococcus geothermalis* to deposits and slimes in paper industry. J. Ind. Microbiol. Biotechnol. **35**:1651–1657.
45. **Peltola M, et al.** 2011. Effects of polarization in the presence and absence of biocides on biofilms in a simulated paper machine water. J. Ind. Microbiol. Biotechnol. **38**:1719–1727.
46. **Prigent-Combaret C, et al.** 2001. Complex regulatory network controls initial adhesion and biofilm formation in *Escherichia coli* via regulation of the *csgD* gene. J. Bacteriol. **24**:7213–7223.
47. **Rasmussen K, Lewandowski Z.** 1997. Microelectrode measurements of local mass transport rates in heterogenous biofilms. Biotechnol. Bioeng. **59**:302–309.
48. **Raulio M, et al.** 2006. Destruction of *Deinococcus geothermalis* biofilm by photocatalytic ALD and sol-gel TiO2 surfaces. J. Ind. Microbiol. Biotechnol. **33**:261–268.
49. **Saarimaa C, et al.** 2006. Characterization of adhesion threads of *Deinococcus geothermalis* as type IV pili. J. Bacteriol. **188**:7016–7021.
50. **Sato A, et al.** 2005. The GTP binding protein Obg homolog ObgE is involved in ribosome maturation. Genes Cells **10**:393–408.
51. **Schmid AK, Howel HA, Battista JR, Peterson SN, Lidstrom ME.** 2005. Global transcriptional and proteomic analysis of the Sig1 heat shock regulon of *Deinococcus radiodurans*. J. Bacteriol. **187**:3339–3351.
52. **Singh R, Lemire J, Mailloux RJ, Appanna VD.** 2008. A novel strategy involved anti-oxidative defense: the conversion of NADH into NADPH by a metabolic network. PLoS One **3**:e2682.
53. **Tian B, et al.** 2010. Proteomic analysis of membrane proteins from a radioresistant and moderate thermophilic bacterium *Deinococcus geothermalis*. Mol. Biosyst. **10**:2068–2077.
54. **Toei M, et al.** 2007. Dodecamer rotor ring defines H^+ /ATP ratio for ATP synthesis of prokaryotic V-ATPase from *Thermus thermophilus*. Proc. Natl. Acad. Sci. U. S. A. **104**:20256–20261.
55. **VanBogelen RA, Schiller EE, Thomas JD, Neidhardt FC.** 1999. Diagnosis of cellular states of microbial organisms using proteomics. Electrophoresis **20**:2149–2159.
56. **Visick JE, Clarke S.** 1995. Repair, refold, recycle: how bacteria can deal with spontaneous and environmental damage to proteins. Mol. Microbiol. **5**:835–845.
57. **Vendeville A, Winzer K, Heurlier K, Tang CM, Hardie KR.** 2005. Making 'sense' of metabolism: autoinducer-2, LuxS, and pathogenic bacteria. Nat. Rev. Microbiol. **3**:383–396.
58. **Väisänen OM, et al.** 1998. Microbial communities of printing paper machines. J. Appl. Microbiol. **84**:1069–1084.
59. **Wagner VE, Bushnell D, Passador L, Brooks AI, Iglewski BH.** 2003. Microarray analysis of *Pseudomonas aeruginosa* quorum-sensing regulons: effects of growth phase and environment. J. Bacteriol. **7**:2080–2095.
60. **Yokoyama K, Oshima T, Yoshida M.** 1990. *Thermus thermophilus* membrane-associated ATPase: indication of a eubacterial V-type ATPase. J. Biol. Chem. **265**:21946–21950.
61. **Zhang YM, Wong TY, Chen LY, Lin CS, Liu JK.** 2000. Induction of a futile Embden-Mayerhof-Parnas pathway in *Deinococcus radiodurans* by Mn: possible role of the pentose phosphate pathway in cell survival. Appl. Environ. Microbiol. **1**:105–112.